Role of Nuclear Chromogranin B in Inositol 1,4,5-Trisphosphate-Mediated Nuclear Ca^{2+} Mobilization

Yang Hoon Huh, Sei Yoon Chu, Seon Young Park, Seong Kwon Huh, and Seung Hyun Yoo*

National Creative Research Initiative Center for Secretory Granule Research and Department of Biochemistry, Inha University College of Medicine, Jung Gu, Incheon 400-712, Korea

Received August 11, 2005; Revised Manuscript Received November 1, 2005

ABSTRACT: Recently, secretory granule Ca^{2+} storage protein chromogranin B (CGB) was shown to be present in the nucleoplasm proper in a complex structure that consists of the inositol 1,4,5-trisphosphate receptor (IP_3R)/Ca^{2+} channels and the phospholipids. Further, the amounts of IP_3Rs present in the nucleus of bovine chromaffin cells were shown to be comparable to that of the endoplasmic reticulum. Therefore, we investigated here the potential contribution of nuclear CGB on the IP_3-dependent Ca^{2+} mobilization in the nucleus, using both neuroendocrine PC12 and nonneuroendocrine NIH3T3 cells. Chromogranin A (CGA) expression in the NIH3T3 cells, which do not contain intrinsic chromogranins, increased the IP_3-induced Ca^{2+} releases in the nucleus by 45%, while CGB expression in the same cells increased the IP_3-induced Ca^{2+} releases in the nucleus by 80%. Microinjection of IP_3 into the nucleus of CGB-expressing NIH3T3 cells increased the IP_3-dependent nuclear Ca^{2+} mobilization ~3-fold, whereas in CGA-expressing cells it remained the same as that of control cells. In contrast, inhibition of CGA expression in PC12 cells by siRNA treatment decreased the IP_3-induced Ca^{2+} releases in the nucleus by 17%, while inhibition of CGB expression decreased the IP_3-induced Ca^{2+} releases in the nucleus by 55%. Microinjection of IP_3 into the nucleus of siCGB-treated PC12 cells decreased the IP_3-dependent nuclear Ca^{2+} mobilization by ~75%, whereas in siCGA-treated cells it remained the same as that of control cells. Given the presence of CGB in the nucleus, these results further highlight the critical contribution of nuclear CGB in the IP_3-induced Ca^{2+} release in the nucleus.

Granin family proteins, chromogranins and secretogranins, are abundantly expressed in neuroendocrine cells, and of these granins chromogranins A and B are the two major proteins of secretory granules of secretory cells (*1*−*6*). Chromogranins are high-capacity, low-affinity Ca^{2+} storage proteins and have been shown to induce secretory granule formation (*7*−*9*), though the granulogenic effect of CGB[1] was 50−60% higher than that of CGA (*8*).

Despite the dominant presence of chromogranins in secretory granules, CGB has also been demonstrated to localize in the nucleus as well (*8*, *10*). The CGB concentration in the secretory granules of bovine adrenal chromaffin cells is estimated to be ~200 μM (*1*) while that in the nucleus ~40−80 μM (*10*). Chromogranin B binds ~90 mol of Ca^{2+}/mol with a dissociation constant of 1.5 mM (*11*). In this regard, the presence of a relatively high CGB concentration in the nucleus implies the existence and operation of a high-capacity Ca^{2+} storage and control system in the nucleus.

Although the IP_3-induced nuclear Ca^{2+} releases have often been attributed to Ca^{2+} releases through the IP_3R/Ca^{2+} channels that are located in the inner nuclear membrane (*12*−*15*), the IP_3R/Ca^{2+} channels have been shown to exist in the nucleoplasm, widely present in both the heterochromatin and the euchromatin regions (*16*, *17*). In adrenal chromaffin cells, it was estimated that ~15% of total cellular IP_3R-1 and -2 and ~25% of total cellular IP_3R-3 are present in the nucleus (*17*). These amounts are comparable to those of IP_3R isoforms present in the endoplasmic reticulum (ER), which were shown to contain ~15−20% of total cellular IP_3Rs (*17*), and point out the potential prominence of IP_3-dependent Ca^{2+} release capacity inside the nucleus.

Moreover, it was further shown that the IP_3Rs, CGB, and phospholipids colocalize in the nucleoplasm, existing in a vesicular nucleoplasmic complex with an estimated average size of ~$(2-3) \times 10^7$ Da (*18*). In light of the presence of the vesicular nucleoplasmic structures that are composed of the IP_3Rs and CGB, it is likely that these structures serve as IP_3-sensitive nucleoplasmic Ca^{2+} stores. The nucleoplasm has been known to contain phosphatidylinositol 4,5-bisphosphate (PIP_2) and phospholipase C (PLC) activity (*19*−*22*), two components that are necessary to produce IP_3. It appears therefore possible for IP_3 to mobilize nucleoplasmic Ca^{2+} in the nucleoplasm by binding and opening the IP_3R/Ca^{2+} channels.

The nucleus is home to chromosomes that were shown to contain 20−32 mM Ca^{2+} depending on the condensation state (*23*); the condensed chromosomes contained higher Ca^{2+} concentrations, whereas the decondensed chromosomes contained lower concentrations. Given 20−32 mM Ca^{2+} in the chromosomes (*23*), it appeared inevitable for high-capacity, low-affinity Ca^{2+} storage proteins such as CGB to actively participate in the control of nuclear Ca^{2+}. Moreover,

* To whom correspondence should be addressed. Tel: 82-32-890-0936. Fax: 82-32-882-0796. E-mail: shyoo@ inha.ac.kr.

[1] Abbreviations: CGB, chromogranin B; IP_3R, inositol 1,4,5-trisphosphate receptor.

10.1021/bi051594r CCC: $33.50
Published on Web 01/07/2006

IP_3-mediated Ca^{2+} release through the IP_3R/Ca^{2+} channel has been shown to be essential in the fusion of nuclear vesicles (*24*). We have hence investigated the effect of nuclear CGB in the control of IP_3-mediated nuclear Ca^{2+} mobilization and found a close relationship between the presence of CGB and the magnitude of IP_3-induced Ca^{2+} mobilization in the nucleus.

EXPERIMENTAL PROCEDURES

Antibodies. Polyclonal anti-rabbit CGA and CGB antibodies were raised against intact bovine CGA and recombinant CGB, and the specificity of these antibodies was confirmed (*8*, *10*, *25*). The antibodies for the ER marker protein calnexin and the nucleus marker protein histone 1 were from Calbiochem and Upstate Biotechnology, respectively.

Construction of Expression Vectors. The expression vectors for CGA and CGB were prepared by polymerase chain reaction (PCR) using bovine cDNA as a template, and the PCR products containing full coding sequences were subcloned into the *Eco*RI/*Xba*I site of pCI-neo mammalian expression vector (Promega), in which transcription of the cloned gene is under the direction of the constitutively active cytomegalovirus promoter. On the other hand, the expression vectors for CGA- and CGB-ECFP were prepared by subcloning the PCR products into the *Nhe*I/*Sal*I site of pd2ECFP-N_1 (Clontech) to produce pd2CGA-ECFP and pd2CGB-ECFP, respectively. Circular plasmid cDNAs for transfection were prepared using the Qiagen maxipreparation kit.

NIH3T3 Cell Culture and Transient Transfection. All culture reagents and powdered media were purchased from Gibco BRL. NIH3T3 cells were maintained in Dulbecco's modified Eagle's medium (DMEM) supplemented with 10% fetal bovine serum. Transient transfection was performed with 70−80% confluent cultures. The cells were transfected with circular plasmid DNAs using LipofecTAMINE-plus transfection reagent (Gibco BRL). Briefly, cells were plated at a density of 5×10^5 cells per well (100 mm in diameter) and were cultured for an additional 24 h. Four micrograms of plasmid DNA in 20 μL of LipofecTAMINE-plus reagent was mixed with 750 μL of OPTI-MEM I medium and incubated for 15 min at room temperature. In addition, 30 μL of LipofecTAMINE reagent was mixed with 750 μL of OPTI-MEM I and incubated for 15 min. The mixture was then added into a culture plate containing 5 mL of OPTI-MEM I medium.

For real time Ca^{2+} release studies, $\sim 5 \times 10^4$ NIH3T3 cells were plated on a glass coverslip in a well containing 800 μL of OPTI-MEM I, and two DNA transfection reagents, reagents 1 and 2, were prepared. Reagent 1 contained 0.1 μg of plasmid DNA in 6 μL of LipofecTAMINE- plus reagent and 100 μL of OPTI-MEM I medium while reagent 2 contained 4 μL of LipofecTAMINE-plus reagent and 100 μL of OPTI-MEM I medium. Both reagents were incubated for 15 min at room temperature, followed by mixing of the two reagents and an additional 15 min of incubation. The mixture was then added to the well containing the cells on a coverslip, and the transfection was performed for 3 h at 37 °C. After transfection, the medium was replaced with fresh prewarmed culture medium and was further incubated for 72 h. In our culture condition, about 70−80% of NIH3T3 cells were transfected. The pCI-neo vector or pd2ECFP-N_1 was used as an empty vector. The transfection of CGA- or CGB-ECFP fusion protein was identified on the basis of the cyan fluorescence emission using 425−445 nm excitation and 460−510 nm emission filters, respectively, and microinjection, Ca^{2+} measurements, and the electron microscope experiments were performed using the successfully transfected cells 48 h after transfection.

PC12 Cell Culture and Transient Transfection of CGA- and CGB-siRNAs. PC12 cells were maintained in RPMI 1640 (Gibco BRL) medium supplemented with 10% fetal bovine serum. Transient siRNA transfection was performed with 70−80% confluent cultures. The CGA-siRNA duplex sense and antisense sequences are 5′-CAACAACAACACAGCAGCUdTdT-3′ and 3′-dTdTGUUGUUGUUGUCGUCGA-5′, respectively, and the CGB-siRNA duplex sense and antisense sequences are 5′-AUGCCCUAUCCAAGUCCAGdTdT-3′ and 3′-dTdTUACGGGAUAGGUUCAGGUC-5′, respectively. The two-nucleotide 3′ overhang of 2′-deoxythymidine is indicated as dTdT. The cells were transfected with the siRNAs using the Silencer siRNA transfection kit (Ambion). Briefly, approximately $1-2 \times 10^6$ PC12 cells were plated on a collagen type IV (BD Biosciences) coated culture dish (100 mm in diameter) in RPMI 1640 medium supplemented with 10% FBS and were cultured for 48 h before transfection. For dose−response experiments of siRNA transfection, 0.25−2 μg of the appropriate siRNA and 10 μL of siPORT Amine were used per 5×10^5 cells. But for the EM study, 1 μg of the appropriate siRNA and 10 μL of siPORT Amine were used per 5×10^5 cells. Addition of more siRNA did not reduce the number of secretory granules further.

For real time Ca^{2+} release studies, $\sim 1 \times 10^5$ PC12 cells were plated on a glass coverslip coated with collagen type IV (BD Biosciences, Palo Alto) in a well containing 800 μL of RPMI 1640 medium supplemented with 10% FBS and were cultured for 48 h before transfection. In preparation of transfection, 6 μL of siPORT Amine was mixed with 194 μL of OPTI-MEM I and incubated for 20 min at room temperature, followed by addition of 0.2 μg of siRNA to the siPORT Amine−OPTI-MEM I mixture for 20 min of additional incubation. The transfection mixture ($\sim$200 μL) was then added into the well containing the cells on a coverslip in 800 μL of RPMI 1640 medium, and the transfection was performed for 6 h at 37 °C. After transfection, the medium was replaced with fresh prewarmed RPMI 1640 medium and was further incubated for 48 h. The transfection was monitored using the Silencer CyTM3 siRNA labeling kit, and the PC12 cells that emitted red fluorescence as determined by using 540/25 nm excitation and 605/55 nm emission filters were considered transfected successfully. Through our siRNA treatments, almost all of the PC12 cells were shown to emit red fluorescence, indicating virtual 100% transfection. Microinjection, Ca^{2+} measurements, and electron microscope experiments were performed using the successfully transfected cells 48 h after transfection.

Detection of Nuclear and Cytosolic Ca^{2+} Signals with Confocal Microscopy. Before incubation with the fluorescent Ca^{2+} indicator, $\sim 5 \times 10^4$ NIH3T3 cells or $\sim 1 \times 10^5$ PC12 cells that had grown on a glass coverslip were stabilized with OPTI-MEM I medium for 30 min. Then the cells were treated with a cell-permeant fluorescent Ca^{2+} indicator fluo-4/AM (4 μM) in OPTI-MEM I for 40 min at 37 °C and 5%

CO_2, after which the cells were washed three times with OPTI-MEM I and then stabilized with the same medium for 30 min at room temperature. The coverslip containing the fluo-4-incubated cells was mounted to a custom-made perfusion chamber on the stage of an inverted microscope (IX71, Olympus). Confocal images of intracellular nuclear and cytosolic Ca^{2+} signals of NIH3T3 and PC12 cells were recorded near the middle of the nucleus using a Perkin-Elmer UltraVIEW LCI confocal imaging system with a 60×, 1.4 NA objective lens. In the case of NIH3T3 cells transfected with CGA- or CGB-ECFP, only the cells that emitted ECFP fluorescence were chosen for Ca^{2+} measurement. To detect the confocal fluorescence images of the calcium signals, fluo-4 was excited at 488 nm using an argon laser and a 488/10 nm excitation filter (Chroma Technology Corp., City, VT), and the emission fluorescence signals were collected through a HQ525/50 nm band-pass filter (Chroma). Images were acquired every 200−400 ms after application of appropriate concentrations of IP_3-producing agonist ATP and every 100 ms after microinjection of 10 nM IP_3 (see below), which were analyzed using the region-of-interest (ROI) function of the UltraVIEW LCI Imaging Suite software 5.0 (Perkin-Elmer, Boston, MA). The Ca^{2+} release in the cytoplasm and nucleus of microinjected cells was measured using the UltraVIEW LCI confocal imaging system with a 100× objective (NA = 1.35) from the optical Z-section transverse the middle region of the nucleus of the cell. In these experiments, only the cells uniformly loaded with fluo-4 fluorescence both in the nucleus and in the cytosol were used.

Microinjection of IP_3. Microinjections were done with an Eppendorf system (Injectman NI2 5181, Femtojet 5247; Eppendorf-Netheler-Hinz, Hamburg, Germany) using pipets (∼100 nm inner diameter) pulled from quartz glass (outer diameter, 1.0 mm; inner diameter, 0.7 mm; Sutter Instrument, Novato, CA) using a P-2000 micropipet puller (Sutter Instrument). The IP_3 to be microinjected were diluted to their final concentration in a buffer (20 mM HEPES, pH 7.2, 110 mM KCl, 2 mM $MgCl_2$, 5 mM KH_2PO_4, 10 mM NaCl) and filtered with a 0.2 μm filter before being filled into the microinjection pipet. Injections were made using the semi-automatic mode of the Eppendorf system at a pipet angle of 45° under the following instrument settings: injection pressure, 80 hPa; compensatory pressure, 60 hPa; injection time, 0.5 s; velocity of the pipet, 2000 μm/s (*26*). Under such conditions using Femtotips II (∼500 nm inner diameter) as pipets, the injection volume had previously been estimated to be 1−1.5% of the cell volume in the case of Jurkat T-lymphocytes (*26*). Hence, in light of the similarity in size between Jurkat T-lymphocytes and PC12 cells, and much larger NIH3T3 cells that have an average diameter ∼3 times larger than that of PC12 cells, our injection volume was also expected to be ∼1% of the PC12 cell volume or less than 0.05% of the NIH3T3 cell volume. Selective microinjection to the nucleus and cytosol was confirmed by microinjection of 4′,6′-diamidino-2-phenylindole (DAPI) and ER-Tracker Blue-White DPX (Molecular Probes, Eugene, OR), respectively. The IP_3-induced Ca^{2+} release was initiated by the microinjection of 10 nM IP_3, and the changes in the fluorescence Ca^{2+} images were acquired every 100 ms.

Ca^{2+} Release as a Function of Time. The fluorescence Ca^{2+} signal (F) of the cells was measured over the regions of interest drawn in the nucleus, nuclear envelope (NE), and cytoplasm. The baseline fluorescence (F_o) of each ROI was calculated as the average fluo-4 fluorescence intensity of 100 frames before IP_3 injection. The onset of the Ca^{2+} signal was determined as the time point at which $F - F_o$ began to rise above 5% of the difference between $F_{max} - F_o$ for the first time.

Extraction of Cellular Proteins and Immunoblot Analysis. To obtain the total cell lysates from the control and siCGA- or siCGB-treated PC12 cells, approximately (4−6) × 10^6 cells were washed twice with ice-cold PBS and lysed in RIPA buffer (50 mM Tris-HCl, pH 8.0, 150 mM NaCl, 5 mM EDTA, 1% NP-40, 1 mM phenylmethanesulfonyl fluoride, and 20 μg/mL aprotinin/leupeptin mix). Then the extracts were incubated for 20 min on ice, and the cell debris was removed by centrifugation at 22000*g* for 10 min at 4 °C. To obtain the cytosolic and nuclear extracts, the harvested cells were lysed by buffer A (10 mM HEPES, pH 7.9, 10 mM KCl, 1 mM EDTA, 1 mM EGTA, 1 mM dithiothreitol, 0.5 mM phenylmethanesulfonyl fluoride, and 0.5% NP-40). The lysates were then incubated for 30 min on ice and then pelleted by centrifugation at 2000*g* for 4 min at 4 °C to separate the cytosolic supernatant and the nuclear pellet. The supernatant was used as the cytosolic proteins. But the nuclear pellet was washed four times with buffer A and was sonicated in a lysis buffer (62.5 mM Tris-HCl, pH 6.8, 1% SDS, 5% glycerol, and 50 mM dithiothreitol) at 4 °C. After incubation for 20 min on ice, the nuclear debris was removed by centrifugation at 21000*g* for 30 min at 4 °C, and the supernatant was used as the nuclear proteins. The proteins (20 or 40 μg each) were then resolved by SDS−PAGE and analyzed by immunoblots using the appropriate antibodies and an ECL detection system (Amersham Life Science).

Immunogold Electron Microscopy. Cells grown on the culture dish were fixed for 1 h at 4 °C in PBS containing 2% glutaraldehyde, 2% paraformaldehyde, and 3.5% sucrose. But the cells intended for immunogold labeling were fixed in the same solution containing 0.1% glutaraldehyde. The cells were then scraped from the culture dish with a cell scraper and pelleted by centrifugation at 2000*g* for 2 min at 4 °C. The cell pellets were resuspended in warm agar (1% in PBS) and repelleted by centrifugation. After three washes in PBS, the agar-embedded cell pellets were postfixed with 1% osmium tetroxide on ice for 2 h, washed three times, and stained en block with 0.5% uranyl acetate, all in PBS. The cell pellets were then embedded in Epon 812 after dehydration in an ethanol series. The ultrathin sections were collected on Formvar/carbon-coated nickel grids and were floated on drops of freshly prepared 3% sodium metaperiodate (*27*) for 30 min. The immunogold labeling procedure was modified from Spector et al. (*28*) and the manufacturer's recommended protocol (British Biocell International, City, U.K.). After etching and washing, the grids were placed on 50 μL droplets of solution A (phosphate saline solution, pH 8.2, containing 4% normal goat serum, 1% BSA, 0.1% Tween 20, and 0.1% sodium azide) for 30 min. Grids were then incubated for 2 h at room temperature in a humidified chamber on 50 μL droplets of anti-rabbit CGA or CGB antibody appropriately diluted in solution B (solution A but with 1% normal goat serum), followed by rinses in solution B. The grids were reacted with 10 nm gold-conjugated goat anti-rabbit IgG diluted in solution A. Controls for the

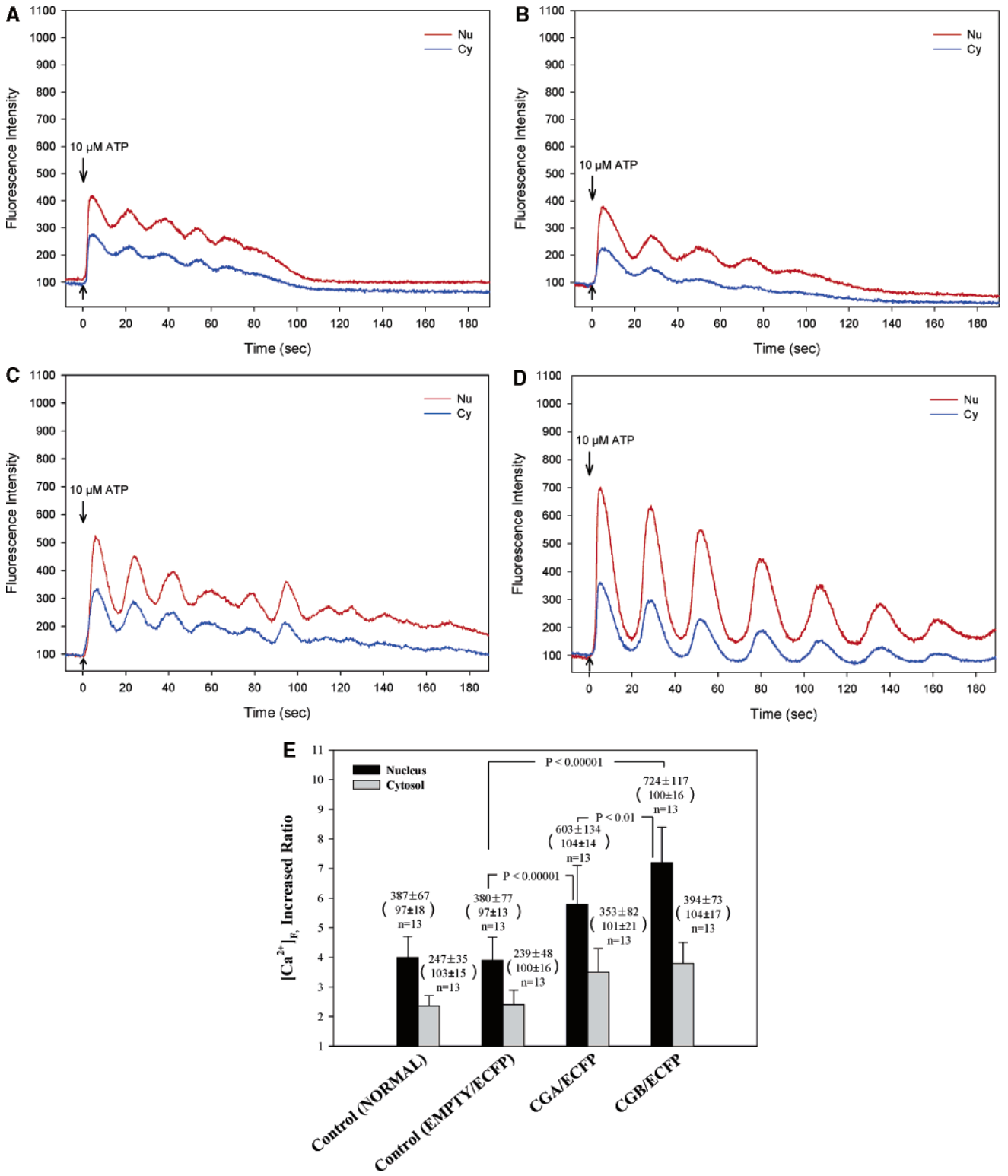

FIGURE 1: IP_3-induced Ca^{2+} mobilization in the nucleus and cytoplasm of NIH3T3 cells. The IP_3-induced Ca^{2+} releases in the nucleus and cytoplasm of NIH3T3 cells, normal (A), empty vector treated (B), transfected with CGA-CFP (C), and transfected with CGB-CFP (D), were measured after stimulation with 10 μM ATP. Traces show the oscillatory fluorescence signals in the nucleus (Nu) and the cytoplasm (Cy) and are representatives of similar results repeated 10−13 times. (E) The highest (top) and baseline (bottom) fluorescence Ca^{2+} signals (means ± SD) are shown in parentheses in each case, and the increases in the fluorescence Ca^{2+} signals are expressed in a bar graph along with the paired *t*-test results.

specificity of CGA and CGB immunogold labeling included (1) omitting the primary antibody and (2) replacing the primary antibody with preimmune serum. After washes in PBS and deionized water, the grids were stained with uranyl acetate (7 min) and lead citrate (2 min) and were viewed with a Zeiss EM912 electron microscope.

RESULTS

IP_3-Induced Intracellular Ca^{2+} Mobilization in NIH3T3 Cells. To determine the effect of chromogranin expression on IP_3-mediated Ca^{2+} mobilization in the nucleus and cytoplasm of NIH3T3 cells, the nonneuroendocrine NIH3T3

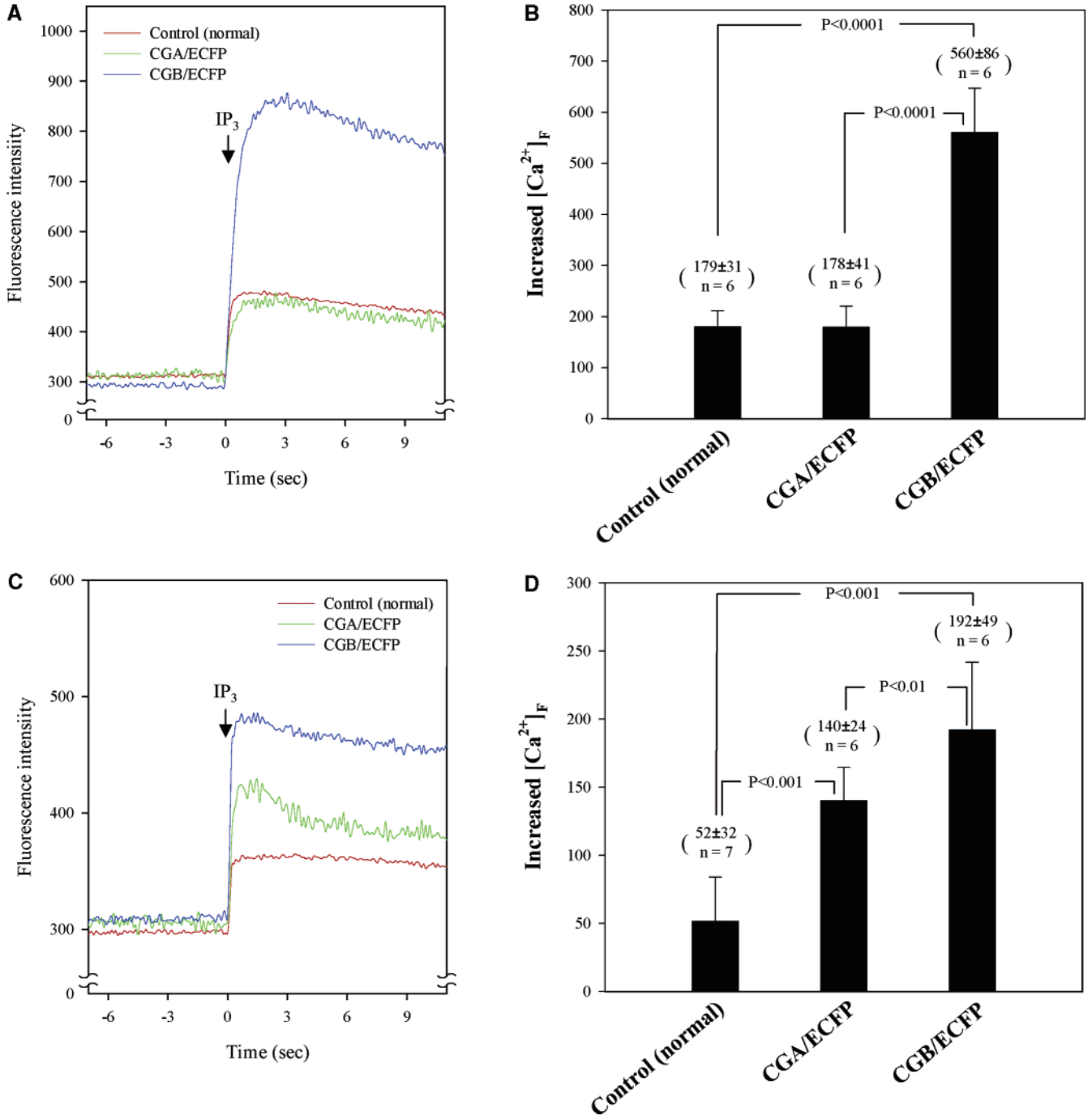

FIGURE 2: Microinjection of IP_3 and Ca^{2+} mobilization in the nucleus and cytoplasm of NIH3T3 cells. The IP_3-induced Ca^{2+} releases in the nucleus of control (normal), CGA-transfected (CGA/ECFP), and CGB-transfected (CGB/ECFP) NIH3T3 cells were measured after microinjection of 10 nM IP_3 into the nucleus of the cell (A). The increases in the fluorescence Ca^{2+} signals (means ± SD) are expressed in a bar graph along with the paired *t*-test results (B). The IP_3-induced Ca^{2+} releases in the cytoplasm of control (normal), CGA-transfected (CGA/ECFP), and CGB-transfected (CGB/ECFP) NIH3T3 cells were also measured after microinjection of 10 nM IP_3 into the cytoplasm of the cell (C). The increases in the fluorescence Ca^{2+} signals are expressed in a bar graph along with the paired *t*-test results (D). Traces show the representative fluorescence signals in the nucleus (A) and the cytoplasm (C), which were repeated six to seven times.

cells that do not express endogenous CGA or CGB were transfected with either CGA-CFP or CGB-CFP, and the expression of CGA and CGB was confirmed (not shown). For $[Ca^{2+}]_i$ measurements of the NIH3T3 cells that had been successfully transfected with either CGA-CFP or CGB-CFP, only the cells that emitted the CFP fluorescence were chosen for $[Ca^{2+}]_i$ measurements.

(A) Application of IP_3-Producing Agonist ATP. The IP_3-mediated Ca^{2+} releases in the nucleus and cytoplasm of normal and chromogranin-expressing NIH3T3 cells were measured using confocal microscopy after application of the IP_3-producing agonist ATP. Figure 1A shows that IP_3 induced oscillatory intracellular Ca^{2+} releases in both the nucleus and cytoplasm of normal NIH3T3 cells, followed by a gradual disappearance of the oscillation. To estimate the magnitude of Ca^{2+} release, the fluorescence Ca^{2+} signal in the first Ca^{2+} peak (highest Ca^{2+} mobilization) was expressed over that of the resting level. This resulted in approximately 4.0-fold (from baseline fluorescence 97 ± 18 to 387 ± 67) and 2.4-fold (from baseline fluorescence 103 ± 15 to 247 ± 35)

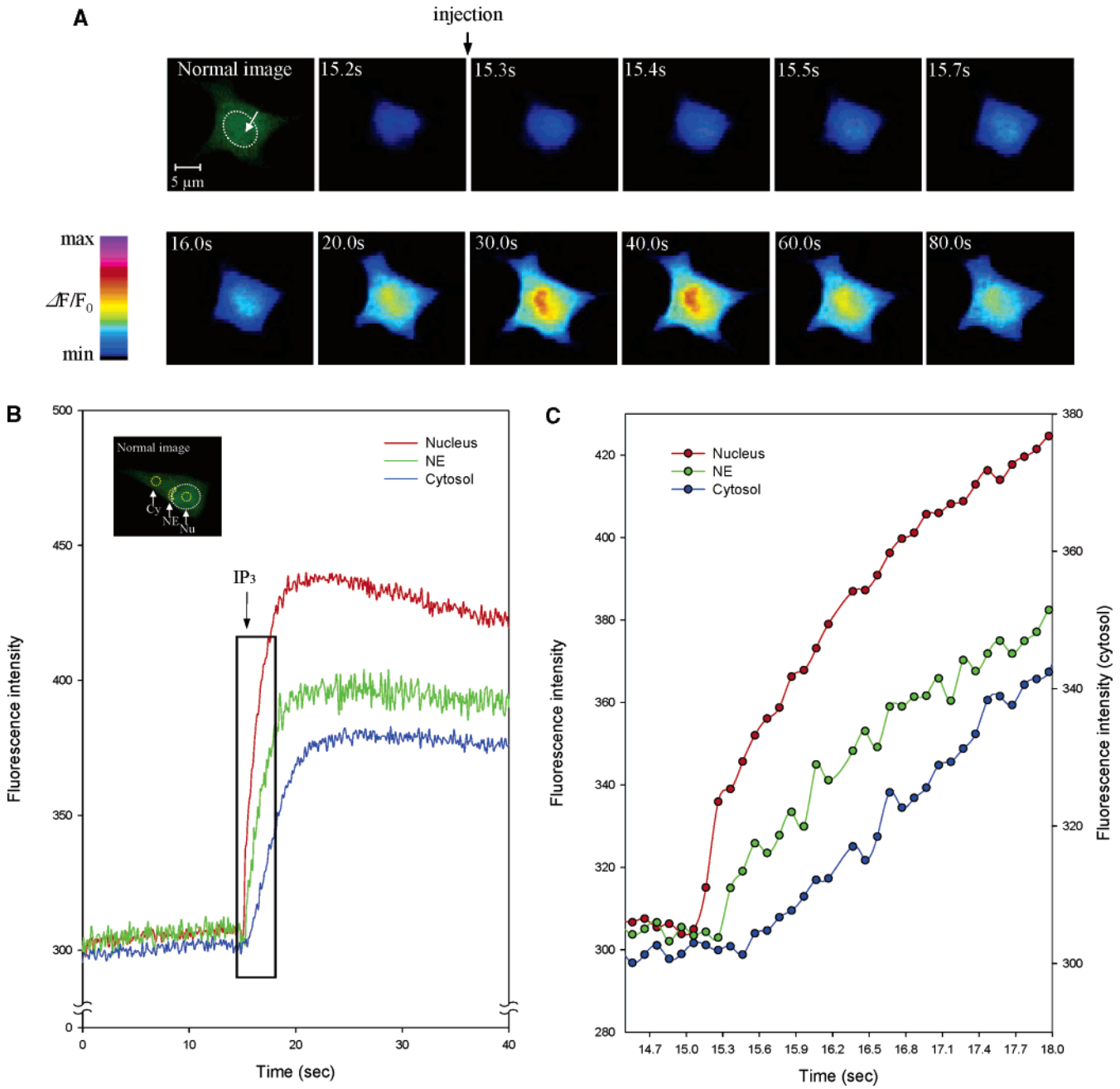

FIGURE 3: Microinjection of IP_3 into the nucleus and Ca^{2+} imaging of NIH3T3 cells. (A) 10 nM IP_3 was microinjected into the nucleus (the exact location of microinjection is indicated by an arrow within the demarked nucleus) of NIH3T3 at the time indicated by a downward arrow (between 15.2 and 15.3 s). The resulting Ca^{2+} release images are shown as a function of time in pseudocolors. Note that the initial IP_3-dependent Ca^{2+} release is limited to the nucleus, though it propagated to the cytoplasm later. (B, C) Temporal resolution of the IP_3-induced Ca^{2+} release shows that Ca^{2+} was released first in the nucleus (Nu), followed by the nuclear envelope (NE) and cytoplasm (Cy) of the NIH3T3 cell injected with IP_3 in the nucleus. The box shown in (B) is redrawn in (C) in an expanded scale. The subcellular regions from which the Ca^{2+} signals were collected are demarked in the normal image. The results shown are typical of cells microinjected with IP_3 in the nucleus.

increases in the initial nuclear and cytoplasmic Ca^{2+} concentrations, respectively, over the resting levels (Figure 1E). Application of same concentration of ATP to the NIH3T3 cells transfected with CFP only (empty vector) also induced oscillatory intracellular Ca^{2+} releases both in the nucleus and in the cytoplasm (Figure 1B), similar to the levels shown in the control cells. This resulted in approximately 3.9-fold (from 97 ± 13 to 380 ± 77) and 2.4-fold (from 100 ± 18 to 239 ± 48) increases in the initial nuclear and cytoplasmic Ca^{2+} concentrations, respectively, over the resting levels (Figure 1E), showing practically no difference between the control cells and the cells transfected with the empty vector.

However, the Ca^{2+} release properties of the nucleus and cytoplasm of chromogranin-expressing NIH3T3 cells were markedly different (Figure 1C,D). IP_3 released significantly larger amounts of Ca^{2+} from the CGA-expressing NIH3T3 cells than the control cells or the cells transfected with the empty vector (Figure 1C), inducing approximately 5.8-fold (from 104 ± 14 to 603 ± 134) and 3.5-fold (from 101 ± 21 to 353 ± 82) increases in the nuclear and cytoplasmic Ca^{2+} concentrations, respectively, over the resting levels (Figure 1E). This result indicates that approximately 45% more nuclear Ca^{2+} and 46% more cytoplasmic Ca^{2+} were released in the CGA-transfected cells than in control cells.

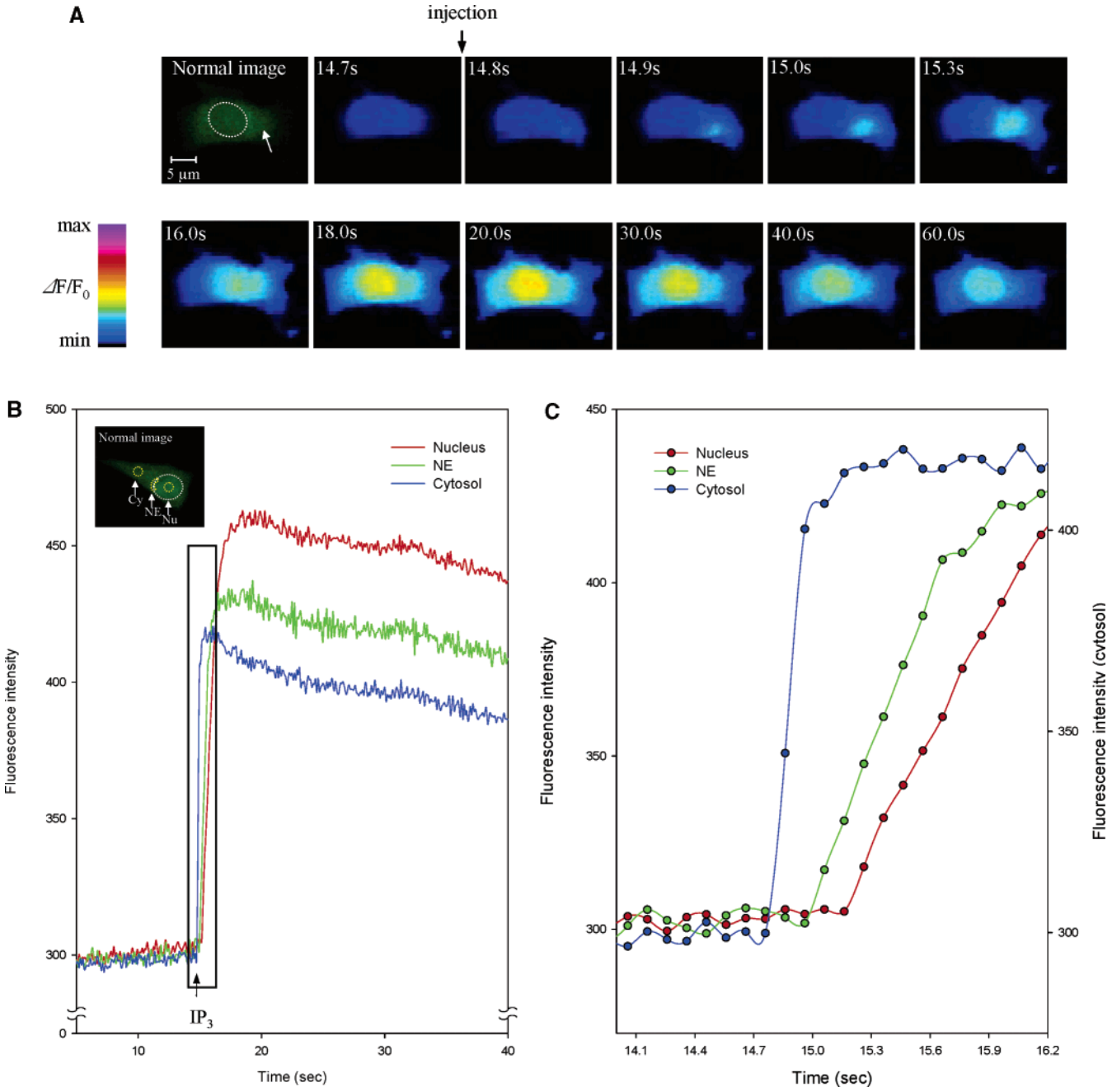

FIGURE 4: Microinjection of IP_3 into the cytoplasm and Ca^{2+} imaging of NIH3T3 cells. (A) 10 nM IP_3 was microinjected into the cytoplasm (the exact location of microinjection is indicated by an arrow outside the demarked nucleus) of NIH3T3 at the time indicated by a downward arrow (between 14.7 and 14.8 s). The resulting Ca^{2+} release images are shown as a function of time in pseudocolors. Note that the initial IP_3-dependent Ca^{2+} release is limited to the cytoplasm, though it propagated to the nucleus later. (B, C) Temporal resolution of the IP_3-induced Ca^{2+} release shows that Ca^{2+} was released first in the cytoplasm (Cy), followed by the nuclear envelope (NE) and nucleus (Nu) of the NIH3T3 cell injected with IP_3 in the cytoplasm. The box shown in (B) is redrawn in (C) in an expanded scale. The subcellular regions from which the Ca^{2+} signals were collected are demarked in the normal image. The results shown are typical of cells microinjected with IP_3 in the cytoplasm.

On the other hand, IP_3 induced markedly higher levels of oscillatory intracellular Ca^{2+} releases in both the nucleus and cytoplasm of CGB-expressing NIH3T3 cells (Figure 1D). In the CGB-expressing cells, IP_3 induced approximately 7.2-fold (from 100 ± 16 to 724 ± 117) and 3.8-fold (from 104 ± 17 to 394 ± 73) increases in the nuclear and cytoplasmic Ca^{2+} concentrations, respectively, over the resting levels (Figure 1E). These amounts of released Ca^{2+} in the CGB-expressing cells represent releases of ~80% and 58% more nuclear and cytoplasmic Ca^{2+} releases, respectively, than the control cells and are even 24% and 8% higher than the respective regions of CGA-expressing cells (Figure 1E). Particularly, the extent of nuclear Ca^{2+} increase, from 45% in the CGA-expressing cells to 80% in the CGB-expressing cells, is significantly greater than the cytoplasmic increase, which increased from 46% to 58%.

(B) Microinjection of IP_3. The effect of nuclear CGB on the IP_3-induced Ca^{2+} release in the nucleus is also demonstrated in the nucleus of NIH3T3 cells by microinjection of IP_3 (Figure 2). As shown in Figure 2A, injection of 10 nM IP_3 into the nucleus of CGB-expressing NIH3T3 cells induced release of markedly larger amounts of nuclear Ca^{2+}

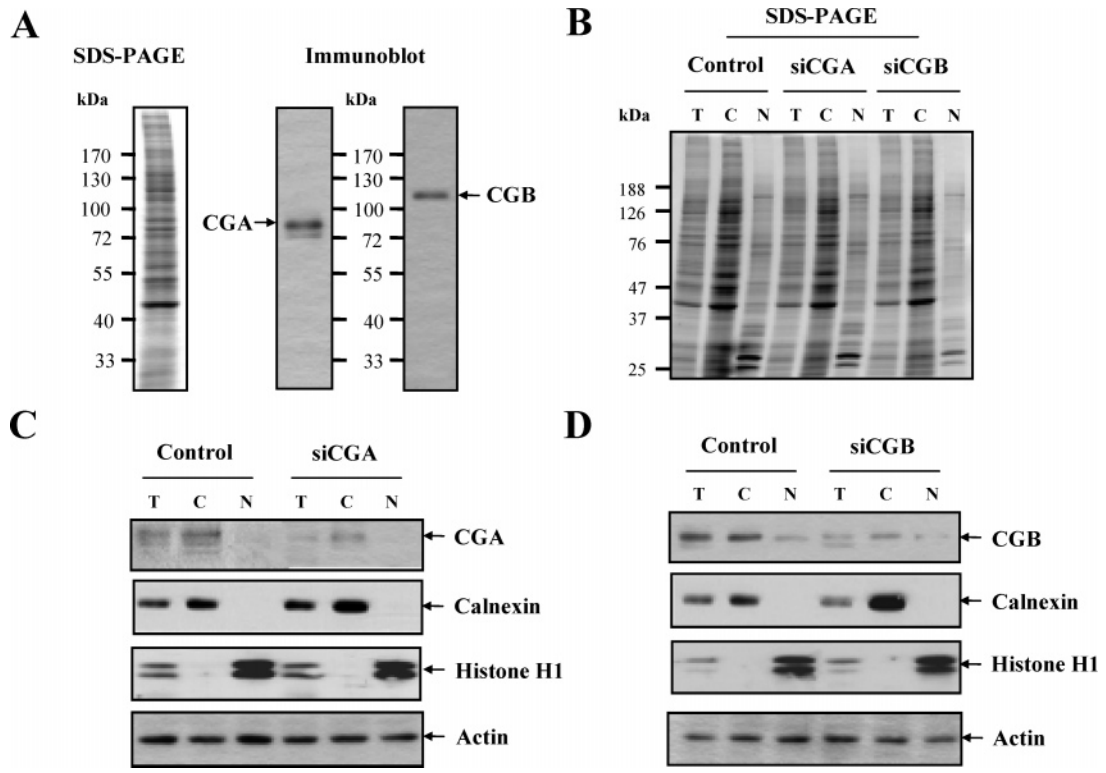

FIGURE 5: Suppression of chromogranin expression in siRNA-treated PC12 cells. (A) Proteins extracted from PC12 cells were separated on a 10% SDS gel (10 μg per lane) and were immunoblotted with CGA (center) and CGB (right) antibodies to confirm the specificity of the antibodies. (B) Proteins from the whole cells (T), the cytoplasm (C), and the nucleus (N) of normal PC12 cells and the cells that had been treated with siCGA- or siCGB-RNA were separated on a 10% SDS gel (5 μg per lane). The same proteins were immunoblotted with CGA (C) and CGB (D) antibodies, along with antibodies for the cytoplasm marker calnexin, the nucleus marker histone H1, and actin (20−40 μg per lane).

compared to those of CGA-expressing or control cells, clearly demonstrating the effect of CGB expression on the IP_3-dependent Ca^{2+} mobilization in the nucleus. The magnitude of IP_3-dependent Ca^{2+} mobilization in the nucleus of CGB-expressing NIH3T3 cells was ~3-fold higher than those of CGA-expressing or control cells (Figure 2A,B). However, injection of 10 nM IP_3 into the nucleus of CGA-expressing NIH3T3 cells induced release of similar amounts of nuclear Ca^{2+} as those released in control cells, indicating that CGA expression does not affect the IP_3-dependent Ca^{2+} mobilization in the nucleus (Figure 2A,B).

However, injection of 10 nM IP_3 into the cytoplasm induced a totally different pattern of Ca^{2+} releases (Figure 2C,D). Unlike the injection into the nucleus, injection of IP_3 into the cytoplasm of CGA-expressing NIH3T3 cells induced IP_3-dependent Ca^{2+} release in the cytoplasm >2-fold compared to that of control cells while injection into the cytoplasm of CGB-expressing cells induced the Ca^{2+} release >3-fold (Figure 2C,D). In view of the expression of both CGA and CGB in the newly formed secretory granules of NIH3T3 cells (8 and Figure 8), these results demonstrate the effects of chromogranins A and B in the control of IP_3-dependent Ca^{2+} mobilization in the cytoplasm (*29*).

To further show that microinjection of IP_3 can clearly distinguish the Ca^{2+} release from the nucleus and cytoplasm, the changes in fluorescence Ca^{2+} signals were shown as a function of time after the IP_3 injection into the nucleus (Figure 3) and cytoplasm (Figure 4). Figure 3A shows the spatiotemporal resolution of Ca^{2+} release of NIH3T3 cells after microinjection of 10 nM IP_3 into the nucleus. The fluorescence Ca^{2+} signal was shown first in the nucleus, which then propagated to the nuclear envelope and onto the rest of the cell (Figure 3A). The temporal differences of the Ca^{2+} releases are shown in the expanded scale in Figure 3B,C, demonstrating the initial release of Ca^{2+} in the nucleus, followed by the NE and the cytoplasm.

On the other hand, the injection of IP_3 into the cytoplasm of NIH3T3 cells induced IP_3-dependent Ca^{2+} release in the cytoplasm first, which later propagated to the nucleus (Figure 4A). The spatiotemporal resolution in expanded scale also shows that injection of IP_3 into the cytoplasm of CGB-expressing NIH3T3 cells induces IP_3-dependent Ca^{2+} mobilization in the cytoplasm first, followed by the NE and nucleus (Figure 4B,C).

IP_3-Induced Nuclear and Cytoplasmic Ca^{2+} Mobilization in PC12 Cells. To determine the effect of chromogranin expression on IP_3-mediated nuclear and cytoplasmic Ca^{2+} mobilizations in neuroendocrine PC12 cells, PC12 cells that express endogenous CGA and CGB were treated with either siCGA- or siCGB-RNA to suppress the expression of either CGA or CGB (Figure 5). To determine the extent of chromogranin suppression in the siCGA- or siCGB-RNA-treated PC12 cells, the protein extracts from total, cytoplasmic, and nuclear fractions of the siRNA-treated cells were separated on an SDS−polyacrylamide gel, and the amounts of CGA and CGB expressed were visualized by immunoblot analyses (Figure 5C,D). Separation of the cytosolic and nuclear proteins was confirmed by immunoblot analyses using antibodies for calnexin, a cytoplasm marker, and histone H1, a nucleus marker. As shown in Figure 5, CGA

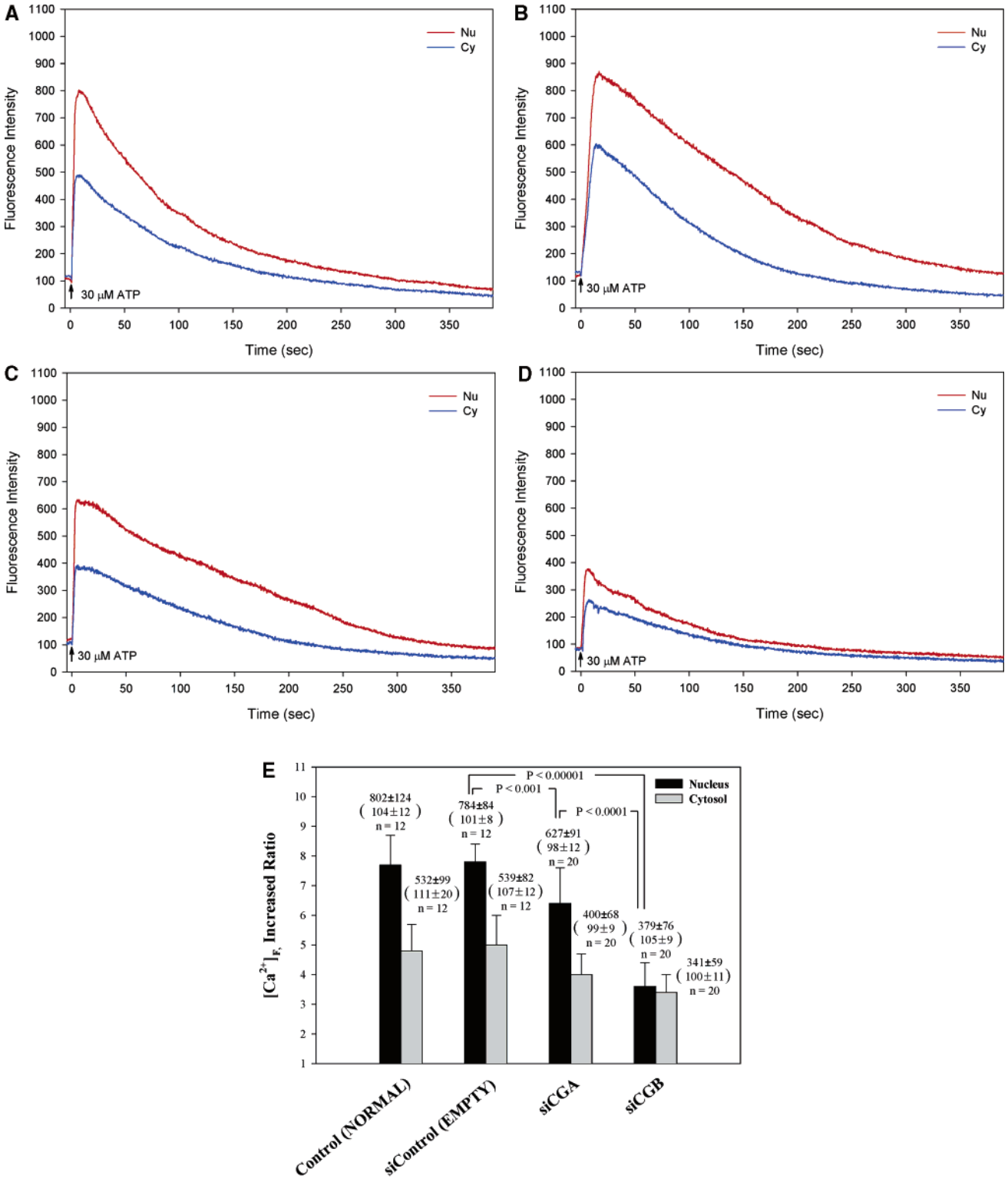

FIGURE 6: IP_3-induced Ca^{2+} mobilization in the nucleus and cytoplasm of PC12 cells. The IP_3-induced Ca^{2+} releases in the nucleus and cytoplasm of PC12 cells, normal (A), empty siRNA treated (B), treated with siCGA (C), and treated with siCGB (D), were measured after stimulation with 30 μM ATP. Traces show the fluorescence signals in the nucleus (Nu) and the cytoplasm (Cy) and are representatives of similar results repeated 10−13 times. (E) The highest (top) and baseline (bottom) fluorescence Ca^{2+} signals (means ± SD) are shown in parentheses in each case, and the increases in the fluorescence Ca^{2+} signals are expressed in a bar graph along with the paired *t*-test results.

was expressed only in the cytoplasm while CGB was expressed in both the cytoplasm and nucleus. Comparison of the control and the siCGA-treated PC12 cells showed that the CGA expression in the siCGA-treated cells was reduced by ~60% in the cytoplasm. Similarly, CGB expression in the siCGB-treated PC12 cells was also reduced by ~60% in both the cytoplasm and the nucleus (Figure 5C,D). Since introduction of siCGA- and siCGB-RNA into PC12 cells has been shown to decrease the expression of CGA and CGB, respectively, in the cells (Figure 5), the effect of reduced

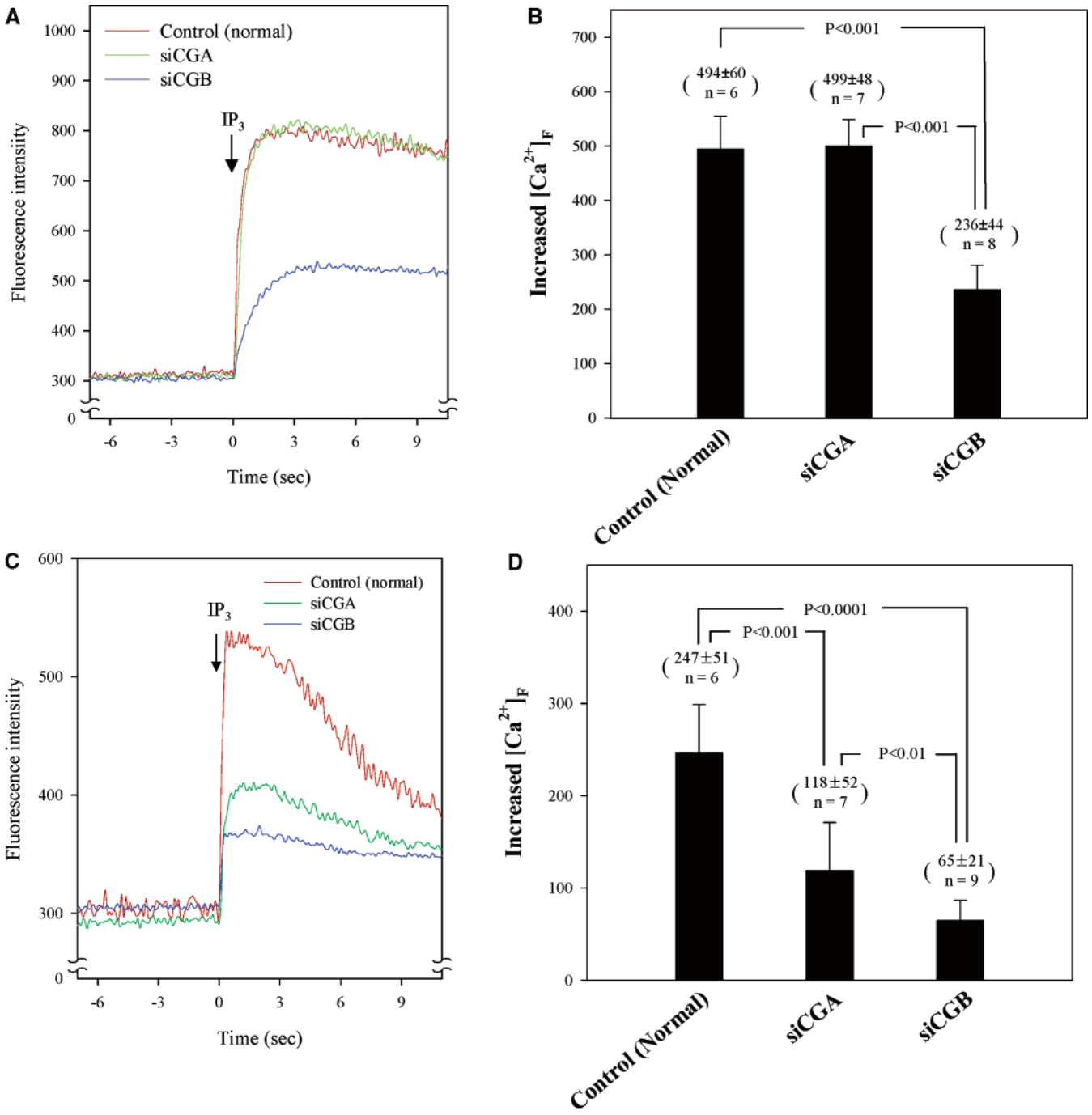

FIGURE 7: Microinjection of IP_3 and Ca^{2+} mobilization in the nucleus and cytoplasm of PC12 cells. (A) The IP_3-induced Ca^{2+} releases in the nucleus of control (normal), siCGA-treated (siCGA), and siCGB-treated (siCGB) PC12 cells were measured after microinjection of 10 nM IP_3 into the nucleus of the cell. (B) The increases in the fluorescence Ca^{2+} signals (mean ± SD) are expressed in a bar graph along with the paired *t*-test results. (C) The IP_3-induced Ca^{2+} releases in the cytoplasm of control (normal), siCGA-treated (siCGA), and siCGB-treated (siCGB) PC12 cells were also measured after microinjection of 10 nM IP_3 into the cytoplasm of the cell. (D) The increases in the fluorescence Ca^{2+} signals (mean ± SD) are expressed in a bar graph along with the paired *t*-test results. Traces show the representative fluorescence signals in the nucleus (A) and the cytoplasm (C), which were repeated six to nine times.

chromogranin expression on IP_3-mediated nuclear and cytoplasmic Ca^{2+} mobilizations was measured in the siRNA-treated PC12 cells.

(A) Application of IP_3-Producing Agonist ATP. As shown in Figure 6, IP_3 induced rapid and steep rises of both the nuclear and cytoplasmic Ca^{2+} concentrations in PC12 cells (Figure 6A), followed by slow sequestrations of the released Ca^{2+}. Unlike the NIH3T3 cells shown in Figure 1, the IP_3-induced oscillatory Ca^{2+} releases were not observed in PC12 cells. IP_3 induced roughly 7.7-fold (from 104 ± 12 to 802 ± 124) and 4.8-fold (from 111 ± 20 to 532 ± 99) increases in the nuclear and cytoplasmic Ca^{2+} concentrations, respectively, over the resting levels (Figure 6E). Application of the same concentration of ATP to the PC12 cells that had gone through the siRNA treatment but without the chromogranin siRNA (empty treatment) also induced rapid and steep rises of both the nuclear and cytoplasmic Ca^{2+} concentrations in the cells (Figure 6B), reaching approximately 7.8-fold (from 101 ± 8 to 784 ± 84) and 5.0-fold (from 107 ± 12 to 539 ± 82) increases of nuclear and

cytoplasmic Ca^{2+} concentrations, respectively, similar to those shown in the control cells (Figure 6E). There was very little difference in the levels of nuclear and cytoplasmic Ca^{2+} mobilized between the control and the empty siRNA-treated cells.

However, when the PC12 cells that had been treated with either siCGA-RNA or siCGB-RNA were exposed to the same stimulation, the amount of intracellular Ca^{2+} released was drastically reduced (Figure 6C,D). When the PC12 cells that had been treated with siCGA-RNA were stimulated with the same concentration of ATP (Figure 6C), the nuclear Ca^{2+} releases increased ~6.4-fold (from 98 ± 12 to 627 ± 91) over the resting levels while the cytoplasmic Ca^{2+} releases increased ~4.0-fold (from 99 ± 9 to 400 ± 68). This amounted to 17% and 16% reductions of the nuclear and cytoplasmic Ca^{2+} releases, respectively, compared to those of control cells (Figure 6E).

Analogous to the effects of reduced CGA expression on the IP_3-induced intracellular Ca^{2+} releases, suppression of CGB expression in PC12 cells also resulted in a marked reduction of the IP_3-mediated nuclear and cytoplasmic Ca^{2+} releases in these cells (Figure 6D). In the PC12 cells that had been treated with the siCGB-RNA, IP_3 induced nuclear and cytoplasmic Ca^{2+} increases of 3.5-fold (from 105 ± 9 to 379 ± 76) and 3.4-fold (from 100 ± 11 to 341 ± 59), respectively, over the resting levels, indicating 55% and 29% reductions of the nuclear and cytoplasmic Ca^{2+}, respectively, compared to those of the control cells (Figure 6E). In particular, the extent of nuclear Ca^{2+} decrease, from 17% in the CGA-suppressed cells to 55% in the CGB-suppressed cells, is significantly greater than corresponding decreases in the cytoplasmic Ca^{2+} releases, which decreased from 16% to 29%.

(B) Microinjection of IP_3. The effect of nuclear CGB on the IP_3-induced Ca^{2+} release in the nucleus is also demonstrated in the nucleus of PC12 cells by microinjection of IP_3 (Figure 7). As shown in Figure 7A, injection of 10 nM IP_3 into the nucleus of siCGA-treated PC12 cells induced release of similar amounts of nuclear Ca^{2+} as those released in control cells, indicating that suppression of intrinsic CGA expression does not affect the IP_3-dependent Ca^{2+} mobilization in the nucleus. However, injection of 10 nM IP_3 into the nucleus of siCGB-treated PC12 cells induced release of markedly smaller amounts of nuclear Ca^{2+} compared to those of siCGA-treated or control cells (Figure 7A), clearly demonstrating the effect of suppression of CGB expression on the IP_3-dependent Ca^{2+} mobilization in the nucleus. The magnitude of IP_3-dependent Ca^{2+} mobilization in the nucleus of siCGB-treated PC12 cells decreased ~55% compared to that of siCGA-treated or control cells (Figure 7B).

However, injection of 10 nM IP_3 into the cytoplasm induces a totally different pattern of Ca^{2+} releases (Figure 7C,D). Unlike the injection into the nucleus, injection of IP_3 into the cytoplasm of siCGA-treated PC12 cells decreased the IP_3-dependent Ca^{2+} release in the cytoplasm ~50% compared to that of control cells (Figure 7C,D). Similarly, injection of IP_3 into the cytoplasm of siCGB-treated PC12 cells decreased the IP_3-dependent Ca^{2+} release in the cytoplasm ~75% compared to that of control cells (Figure 7C,D). In view of intrinsic expression of both CGA and CGB in secretory granules of PC12 cells, these results also demonstrate the effects of chromogranins A and B in the control of IP_3-dependent Ca^{2+} mobilization in the cytoplasm (*29*). Nevertheless, the effects CGA and CGB on the IP_3-dependent Ca^{2+} release in the nucleus were clearly different (Figure 7A,B); only CGB was effective in the control of IP_3-induced Ca^{2+} mobilization in the nucleus.

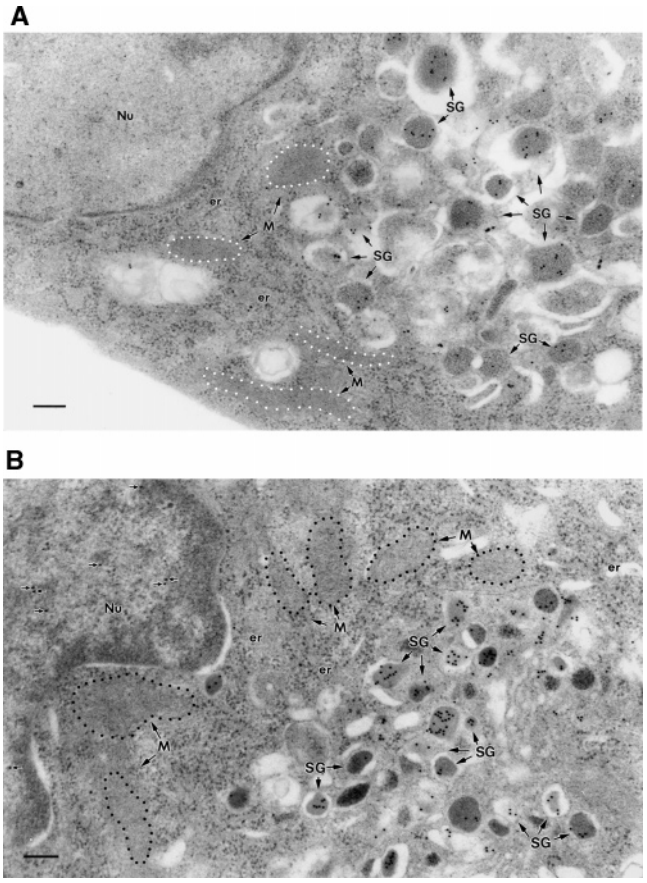

FIGURE 8: Immunogold electron microscopy showing the localization of chromogranins in NIH3T3 cells transfected with chromogranins. Nonneuroendocrine NIH3T3 cells that had been transfected with CGA were immunolabeled for CGA (A), and those transfected with CGB were immunolabeled for CGB (B) (10 nm gold) with the affinity-purified CGA or CGB antibody. The CGA- or CGB-labeling gold particles are localized in the endoplasmic reticulum (er) and secretory granules (SG) but not in mitochondria (M). However, only the CGB-labeling gold particles (indicated by arrows) are localized in the nucleus (Nu). Bar = 200 nm.

Immunogold Electron Microscopy of CGA and CGB. To determine the localization and relative density of the chromogranins in subcellular organelles of chromogranin-expressing NIH3T3 cells and PC12 cells, CGA- or CGB-labeling immunogold electron microscopy was used. Figure 8 shows the localization of CGA (Figure 8A) and CGB (Figure 8B) in chromogranin-expressing NIH3T3 cells. Since CGA and CGB induce de novo secretory granule formation in nonneuroendocrine cells (*7*−*9*), the chromogranin-expressing NIH3T3 cells contain secretory granules (Figure 8). The CGA-labeling immunogold particles were localized in secretory granules and the endoplasmic reticulum (ER) of the NIH3T3 cells but not in the mitochondria or the nucleus (Figure 8A). This indicated that secretory granules formed in the CGA-expressing NIH3T3 cells also contain CGA, as has been the case with secretory granules of neuroendocrine cells (*8*). But no CGA was detected in the nucleus as reported before (*10*).

Table 1: Distribution of the CGA- and CGB-Labeled Gold Particles in CGA- and CGB-Transfected NIH3T3 Cells

	CGA		CGB	
	no. of gold particles[a]/ area viewed (μm^2)	gold particles/μm^2	no. of gold particles[b]/ area viewed (μm^2)	gold particles/μm^2
secretory granule	342/5.85	58.5	334/6.29	53.1
nucleus	7/15.82	0.4	123/26.10	17.4
endoplasmic reticulum	69/11.76	5.9	67/13.10	5.1
mitochondria	3/2.61	1.1	4/2.42	1.7

[a] Ten images from five different tissue preparations were used. [b] Ten images from four different tissue preparations were used.

As shown in Table 1, the number of CGA-labeling gold particles in secretory granules and the ER was 58.5/μm^2 and 5.9/μm^2, respectively, whereas that in the nucleus was 0.4/μm^2. Since the number of CGA-labeling gold particles in the mitochondria was 1.1/μm^2, a number indicative of background level, the number of gold particles found in the nucleus was below the background level, indicating the absence of CGA in the nucleus. Therefore, even taking the background into consideration, 58.5 CGA gold particles/μm^2 in secretory granules is ~10 times higher than 5.9 CGA gold particles/μm^2 in the ER.

In contrast, CGB has previously been found to localize in the nucleus (*10*) in addition to the usual localization in secretory granules and the endoplasmic reticulum. Indeed, the CGB-labeling immunogold particles were shown to localize in the nucleus of the CGB-expressing NIH3T3 cells in addition to secretory granules and the ER (Figure 8B). The number of CGB-labeling gold particles localized in secretory granules and the ER was 53.1/μm^2 and 5.1/μm^2, respectively, while that of the nucleus was 17.4/μm^2. In light of 1.7 CGB-labeling gold particles/μm^2 in the mitochondria, 17.4 CGB-labeling gold particles/μm^2 in the nucleus represents ~30% of the CGB concentration shown in secretory granules and clearly indicates the presence of CGB in the nucleus. Similar to CGA, 53.1 CGB gold particles/μm^2 in secretory granules is ~10 times higher than 5.1 CGB gold particles/μm^2 in the ER.

The distribution and relative density of intrinsic chromogranins A and B in PC12 cells were also examined using immunogold electron microscopy (Figure 9). The CGA- and CGB-labeling gold particles were found in secretory granules and the ER (Figure 8), whereas in the nucleus only the CGB-labeling gold particles were found (Figure 8B), demonstrating the presence of CGB in the nucleus. The number of CGA-labeling immunogold particles in secretory granules of control PC12 cells was 91.1/μm^2 while that of the siCGA-treated cells was 78.6/μm^2 (Table 2), showing a 13.7% reduction in the amount of CGA present in secretory granules of the siCGA-treated cells. Despite a substantial reduction, ~41% reduction (*10*), of the number of secretory granules in siCGA-treated PC12 cells, the difference in the amounts of CGA present in secretory granules of normal and siCGA-treated PC12 cells did not appear to be large. This might be due to the granulogenic role of CGA; perhaps a certain amount of CGA is required before a secretory granule can be formed. As reported before (*10*), CGA was shown to be absent in the nucleus (Figure 9A), and the few CGA-labeling gold particles found in the nucleus were regarded to be backgrounds.

Likewise, the number of CGB-labeling immunogold particles in secretory granules of control PC12 cells was 96.2/μm^2 while that of the siCGB-treated cells was 81.8/μm^2 (Table 3), showing a 15.0% reduction in the amount of CGB present in secretory granules of siCGB-treated cells. SiCGB treatment reduced the number of secretory granules in PC12 cells ~78% (*10*). Nevertheless, there were only 15% less CGB in the secretory granules of siCGB-treated PC12 cells compared to those of normal cells. Similar to siCGA-treated cells, perhaps there exists a minimum requirement for a fixed amount of CGB whether the expression is suppressed by siRNA treatment or not before a secretory granule can be formed in the trans-Golgi network. However, unlike CGA which was not expressed in the nucleus, CGB was expressed

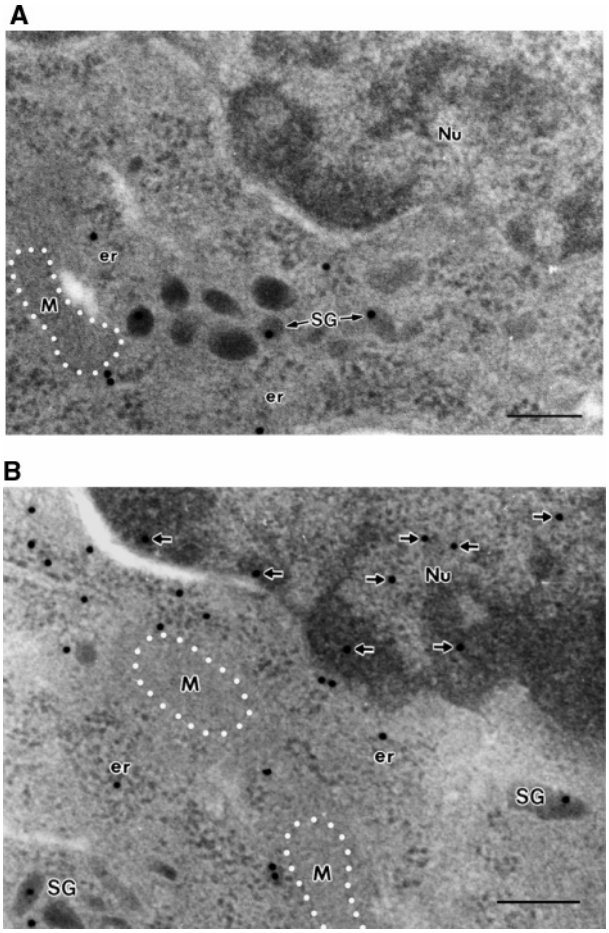

FIGURE 9: Immunogold electron microscopy showing the localization of chromogranins in PC12 cells. Neuroendocrine PC12 cells contain intrinsic chromogranins. The CGA-labeling (A) and CGB-labeling (B) gold particles (15 nm gold) in normal PC12 cells are shown. The CGA- or CGB-labeling gold particles are localized in the endoplasmic reticulum (er) and secretory granules (SG) but not in mitochondria (M). However, the CGB-labeling gold particles (indicated by arrows) are localized in the nucleus (Nu) as well (B). Bar = 200 nm.

Table 2: Distribution of the CGA-Labeling Gold Particles in PC12 Cells

	normal PC12		CGA-siRNA-transfected PC12	
	no. of gold particles[a]/ area viewed (μm^2)	gold particles/μm^2	no. of gold particles[b]/ area viewed (μm^2)	gold particles/μm^2
secretory granule	51/0.56	91.1	11/0.14	78.6
nucleus	5/5.75	0.9	3/3.59	0.8
mitochondria	0/0.90	0.0	0/0.86	0.0

[a] Seventeen images were used. [b] Ten images were used.

Table 3: Distribution of the CGB-labeling Gold Particles in PC12 Cells

	normal PC12		CGB-siRNA-transfected PC12	
	no. of gold particles[a]/ area viewed (μm^2)	gold particles/μm^2	no. of gold particles[b]/ area viewed (μm^2)	gold particles/μm^2
secretory granule	75/0.78	96.2	9/0.11	81.8
nucleoplasm	164/10.76	15.2	29/4.04	7.2
mitochondria	0/0.76	0.0	0/0.83	0.0

[a] Eighteen images were used. [b] Ten images were used.

in the nucleus (Figure 9B). The number of CGB-labeling gold particles in the nucleus was 15.2/μm^2 in control PC12 cells but decreased to 7.2/μm^2 in the siCGB-treated cells (Table 3), indicating a reduction of 47% as a result of the siCGB treatment.

DISCUSSION

Present results show that the presence of chromogranin A or chromogranin B in both neuroendocrine PC12 cells and nonneuroendocrine NIH3T3 cells significantly changes the IP_3-induced intracellular Ca^{2+} mobilization capacities of the cells. The cytoplasmic Ca^{2+} increases in CGB-expressing NIH3T3 cells (58%) were slightly higher than those of CGA-expressing cells (46%). But the extent of IP_3-induced nuclear Ca^{2+} increases in CGB-expressing NIH3T3 cells (80%) was considerably higher than that of the nuclear Ca^{2+} increases in CGA-expressing cells (45%). In light of the presence of CGB, but not CGA, in the nucleus, the marked difference (35%) in the amount of nuclear Ca^{2+} mobilized appeared to point out the contribution of nuclear CGB. The presence of CGA or CGB in the cytoplasm of NIH3T3 cells increased the amount of cytoplasmic Ca^{2+} mobilized in response to IP_3 by 46−58%. Given the presence of ~80 μM CGB in the nucleus (*30*), the greater mobilization of IP_3-induced nuclear Ca^{2+} in the CGB-expressing cells than in CGA-expressing cells suggested an apparent contribution of nuclear CGB in the IP_3-mediated nuclear Ca^{2+} mobilization.

Since CGB is a high-capacity, low-affinity Ca^{2+} storage protein that is capable of binding ~90 mol of Ca^{2+}/mol with a dissociation constant of 1.5 mM (*11*), it is quite likely that nuclear CGB, which exists at ~80 μM in the nucleus (*30*), play a pivotal role in controlling nuclear Ca^{2+} concentration. From the fact that there were no apparent differences in the morphology of the nucleus between the CGA-suppressed or CGB-suppressed PC12 cells, the reduced level of IP_3-induced nuclear Ca^{2+} releases in the CGB-suppressed cells appeared to reflect the reduction of the overall Ca^{2+} storage/control capacity of the nucleus. Moreover, in view of the observation that the presence of CGB in the cell dictated the amount of Ca^{2+} mobilized in response to IP_3 (*29*), the IP_3-induced nuclear Ca^{2+} mobilization indicated a close connection between CGB and the IP_3Rs in the nucleus.

Indeed, all three IP_3R isoforms have been demonstrated to exist in the nucleoplasm of both neuroendocrine chromaffin cells and nonneuroendocrine NIH3T3 cells (*16*, *17*). Moreover, of particular interest was the fact that the nucleus contained ~15% of total cellular IP_3R-1 and -2 and ~25% of total cellular IP_3R-3 while the ER contained ~15−20% of each of the three cellular IP_3R isoforms (*17*). In addition, the concentrations of IP_3R-1 and -2 in the nucleus were slightly lower than those of the ER while the nuclear IP_3R-3 concentration was higher than that of the ER (*17*). These results revealed for the first time that the nucleus has the necessary machinery to function as one of the major IP_3-sensitive intracellular Ca^{2+} stores.

In this respect, the presence of CGB in the nucleus further strengthens the status of the nucleus as a subcellular organelle that can store and release a large share of intracellular Ca^{2+} that can be mobilized by IP_3. This is particularly so given that chromogranins A and B have been shown to interact with the IP_3Rs (*31*) and to activate the IP_3R/Ca^{2+} channels (*32*−*34*). Chromogranin A increased the open probability of the channel by 9-fold and the mean open time by 12-fold (*33*) while CGB increased the open probability and the mean open time by 16-fold and 42-fold, respectively, at the intragranular pH 5.5 (*34*). Yet the channel-activating effect of CGA disappeared at a near physiological pH 7.5 due to its dissociation from the IP_3Rs at that pH (*32*, *33*). But unlike CGA that dissociated from the IP_3R at pH 7.5, CGB nonetheless maintained interaction with the IP_3Rs even at pH 7.5 and activated the IP_3R/Ca^{2+} channel (*32*), increasing the open probability and the mean open time of the IP_3R/Ca^{2+} channel by 8-fold and 23-fold, respectively (*34*).

Next to secretory granules that were shown to contain ~60−70% of total cellular IP_3R isoforms (*17*) and ~200 μM CGB (*1*), the ER was also estimated to contain ~120 μM CGB (*30*), explaining the role of the ER as an important IP_3-sensitive intracellular Ca^{2+} store. As expected, the functional coupling between CGB and the IP_3R/Ca^{2+} channels in the ER has been shown to be critical in the IP_3-mediated Ca^{2+} release from the ER (*35*). Disruption of the coupling between CGB and the IP_3R/Ca^{2+} channels in the ER resulted in severe reduction of the IP_3-mediated Ca^{2+} release from the ER (*35*), demonstrating the functional

importance of the coupling in the storage and release of Ca^{2+} in the ER. Hence, considering the amounts of the IP_3Rs and CGB that exist in the ER and nucleus, the IP_3-dependent Ca^{2+} mobilization capability of the nucleus in the cell is expected to be comparable to that of the ER. The essential role of CGB in IP_3-dependent intracellular Ca^{2+} mobilization has also been shown in EGF-differentiated PC12 cells and hippocampal neurons that the initial intracellular Ca^{2+} release in these cells occurred first in the regions where CGB is localized (*36*).

The present results highlight distinct roles of CGB in the IP_3-mediated Ca^{2+} mobilization in the nucleus. Despite many similarities in biochemical properties of chromogranins A and B, the nuclear localization is the exclusive property of CGB, and this seems to underscore the Ca^{2+} controlling role of CGB in the nucleus. It is therefore natural to postulate that the role of nuclear CGB is to control the nuclear IP_3R/Ca^{2+} channels via its coupling to the IP_3Rs (*31*). In particular, given the high-capacity, low-affinity Ca^{2+} storage capability of CGB (*11*), the highly efficient IP_3R/Ca^{2+} channel-activating role of CGB (*34*) will be of critical use in controlling the nuclear calcium.

ACKNOWLEDGMENT

We thank J. Y. Ghee and S. J. Bahk for help in the experiments.

REFERENCES

1. Winkler, H., and Fischer-Colbrie, R. (1992) The chromogranins A and B: the first 25 years and future perspectives, *Neuroscience 49*, 497−528.
2. Huttner, W. B., Gerdes, H. H., and Rosa, P. (1990) The granin (chromogranin/secretogranin) family, *Trends Biochem. Sci. 16*, 27−30.
3. Iacangelo, A. L., and Eiden, L. E. (1995) Chromogranin A: current status as a precursor for bioactive peptides and a granulogenic/sorting factor in the regulated secretory pathway, *Regul. Pept. 58*, 65−88.
4. Helle, K. B. (2000) The chromogranins. Historical perspectives, *Adv. Exp. Med. Biol. 482*, 3−20.
5. Aunis, D., and Metz-Boutigue, M. H. (2000) Chromogranins: Current concepts. Structural and functional aspects, *Adv. Exp. Med. Biol. 482*, 21−38.
6. Taupenot, L., Harper, K. L., and O'Connor, D. T. (2003) The chromogranin-secretogranin family, *N. Engl. J. Med. 348*, 1134−1149.
7. Kim, T., Tao-Cheng, J. H., Eiden, L. E., and Loh, Y. P. (2001) Chromogranin A, an on/off switch controlling dense-core secretory granule biogenesis, *Cell 106*, 499−509.
8. Huh, Y. H., Jeon, S. H., and Yoo, S. H. (2003) Chromogranin B-induced secretory granule biogenesis: Comparison with the similar role of chromogranin A, *J. Biol. Chem. 278*, 40581−40589.
9. Beuret, N., Stettler, H., Renold, A., Rutishauser, J., and Spiess, M. (2004) Expression of regulated secretory proteins is sufficient to generate granule-like structures in constitutively secreting cells, *J. Biol. Chem. 279*, 20242−20249.
10. Yoo, S. H., You, S. H., Kang, M. K., Huh, Y. H., Lee, C. S., and Shim, C. S. (2002) Localization of secretory granule marker protein chromogranin B in the nucleus: Potential role in transcription control, *J. Biol. Chem. 277*, 16011−16021.
11. Yoo, S. H., Oh, Y. S., Kang, M. K., Huh, Y. H., So, S. H., Park, H. S., and Park, H. Y. (2001) Localization of three subtypes of the inositol 1,4,5-trisphosphate receptor/Ca^{2+} channel in the secretory granules and coupling with the Ca^{2+} storage proteins chromogranins A and B, *J. Biol. Chem. 276*, 45806−45812.
12. Gerasimenko, O. V., Gerasimenko, J. V., Tepikin, A. V., and Petersen, O. H. (1995) ATP-dependent accumulation and inositol trisphosphate or cyclic ADP-ribose-mediated release of Ca^{2+} from the nuclear envelope, *Cell 80*, 439−444.
13. Leite, M. F., Thrower, E. C., Echevarria, W., Koulen, P., Hirata, K., Bennett, A. M., Ehrlich, B. E., and Nathanson, M. H. (2003) Nuclear and cytosolic calcium are regulated independently, *Proc. Natl. Acad. Sci. U.S.A. 100*, 2975−2980.
14. Stehno-Bittel, L., Perez-Terzic, C., and Clapham, D. E. (1995) Diffusion across the nuclear envelope inhibited by depletion of the nuclear Ca^{2+} store, *Science 270*, 1835−1838.
15. Humbert, J. P., Matter, N., Artault, J. C., Köppler, P., and Malviya, A. N. (1996) Inositol 1,4,5-trisphosphate receptor is located to the inner nuclear membrane vindicating regulation of nuclear calcium signaling by inositol 1,4,5-trisphosphate, *J. Biol. Chem. 271*, 478−485.
16. Huh, Y. H., and Yoo, S. H. (2003) Presence of the inositol 1,4,5-trisphosphate receptor isoforms in the nucleoplasm, *FEBS Lett. 555*, 411−418.
17. Huh, Y. H., Yoo, J. A., Bahk, S. J., and Yoo, S. H. (2005) Distribution profile of inositol 1,4,5-trisphosphate receptor isoforms in adrenal chromaffin cells, *FEBS Lett. 579*, 2597−2603.
18. Yoo, S. H., Nam, S. W., Huh, S. K., Park, S. Y., and Huh, Y. H. (2005) Presence of a nucleoplasmic complex composed of the inositol 1,4,5-trisphosphate receptor/Ca^{2+} channel, chromogranin B, and phospholipids, *Biochemistry 44*, 9246−9254.
19. Divecha, N., Banfic, H., and Irvine, R. F. (1991) Inositides and the nucleus and inositides in the nucleus, *Cell 74*, 405−407.
20. Divecha, N., Rhee, S. G., Letcher, A., and Irvine, R. F. (1993) Phosphoinositide signaling enzymes in rat liver nuclei: phosphoinositidase C isoform β is specifically, but not predominantly located in the nucleus, *Biochem. J. 289*, 617−620.
21. D'Santos, C. S., Clarke, J. J., and Divecha, N. (1998) Phospholipid signaling in the nucleus, *Biochim. Biophys. Acta 1436*, 201−232.
22. Irvine, R. F. (2003) Nuclear lipid signaling, *Nat. Rev. Mol. Cell Biol. 4*, 349−360.
23. Strick, R., Strissel, P. L., Gavrilov, K., and Levi-Setti, R. (2001) Cation-chromatin binding as shown by ion microscopy is essential for the structural integrity of chromosomes, *J. Cell Biol. 155*, 899−910.
24. Sullivan, K. M. C., Busa, W. B., and Wilson, K. L. (1993) Calcium mobilization is required for nuclear vesicle fusion in vitro: Implications for membrane traffic and IP_3 receptor function, *Cell 73*, 1411−1422.
25. Park, H. Y., So, S. H., Lee, W. B., You, S. H., Kang, M. K., and Yoo, S. H. (2002) Purification, pH-dependent conformational change, aggregation, and secretory granule membrane binding property of secretogranin II (chromogranin C), *Biochemistry 41*, 1259−1266.
26. Guse, A. H., Berg, I., da Silva, C. P., Potter, B. V., and Mayr, G. W. (1997) Ca^{2+} entry induced by cyclic ADP-ribose in intact T-lymphocytes, *J. Biol. Chem. 272*, 8546−8550.
27. Murphy, S. M., Pilowsky, P. M., and Llewellyn-Smith, I. J. (1998) Pre-embedding staining for GAD67 versus postembedding staining for GABA as markers for central GABAergic terminals, *J. Histochem. Cytochem. 46*, 1261−1268.
28. Spector, D. L., Fu, X. D., and Maniatis, T. (1991) Associations between distinct pre-messenger-RNA splicing components and the cell-nucleus, *EMBO J. 10*, 3467−3481.
29. Huh, Y. H., Jeon, S. H., Yoo, J. A., Park, S. Y., and Yoo, S. H. (2005) Effects of chromogranin expression on the inositol 1,4,5-trisphosphate-induced intracellular Ca^{2+} mobilization, *Biochemistry 44*, 6122−6132.
30. Huh, Y. H., Bahk, S. J., Ghee, J. Y., and Yoo, S. H. (2005) Subcellular distribution of chromogranins A and B in bovine adrenal chromaffin cells, *FEBS Lett. 579*, 5145−5151.
31. Yoo, S. H., So, S. H., Kweon, H. S., Lee, J. S., Kang, M. K., and Jeon, C. J. (2000) Coupling of the inositol 1,4,5-trisphosphate receptor and chromogranins A and B in secretory granules, *J. Biol. Chem. 275*, 12553−12559.
32. Yoo, S. H., and Jeon, C. J. (2000) Inositol 1,4,5-trisphosphate receptor/Ca^{2+} channel modulatory role of chromogranin A, a Ca^{2+} storage protein of secretory granules, *J. Biol. Chem. 275*, 15067−15073.
33. Thrower, E. C., Park, H. Y., So, S. H., Yoo, S. H., and Ehrlich, B. E. (2002) Activation of the inositol 1,4,5-trisphosphate receptor by the Ca^{2+} storage protein chromogranin A, *J. Biol. Chem. 277*, 15801−15806.
34. Thrower, E. C., Choe, C. U., So, S. H., Jeon, S. H., Ehrlich, B. E., and Yoo, S. H. (2003) A functional interaction between

chromogranin B and the inositol 1,4,5-trisphosphate receptor/Ca^{2+} channel, *J. Biol. Chem. 278*, 49699−49706.
35. Choe, C. U., Harrison, K. D., Grant, W., and Ehrlich, B. E. (2004) Functional coupling of chromogranin with the inositol 1,4,5-trisphosphate receptor shapes calcium signaling, *J. Biol. Chem. 279*, 35551−35556.
36. Jacob, S. N., Choe, C. U., Uhlen, P., DeGray, B., Yeckel, M. F., and Ehrlich, B. E. (2005) Signaling microdomains regulate inositol 1,4,5-trisphosphate-mediated intracellular calcium transients in cultured neurons, *J. Neurosci. 25*, 2853−2864.

BI051594R